HSV-2 glycoprotein J promotes viral protein expression and virus spread

Yalan Liu[1], Xinmeng Guan[1,2], Chuntian Li[1,2], Fengfeng Ni[1,2], Sukun Luo[4], Jun Wang[4], Di Zhang[1,2], Mudan Zhang[1], Qinxue Hu[1,3#]

[1]State Key Laboratory of Virology, Wuhan Institute of Virology, Chinese Academy of Sciences, Wuhan 430071, China

[2]University of Chinese Academy of Sciences, Beijing 100049, China

[3]Institute for Infection and Immunity, St George's University of London, London, SW17 0RE, UK

[4]Wuhan Children's Hospital (Wuhan Maternal and Child Healthcare Hospital), Tongji Medical College, Huazhong University of Science & Technology, China

Running title: HSV-2 gJ promotes virus protein expression and spread

[#]Corresponding author: Qinxue Hu. State Key Laboratory of Virology, Wuhan Institute of Virology, Chinese Academy of Sciences, Wuhan 430071, China. E-mail: qhu@wh.iov.cn, Telephone: +86 27 87199992, Fax: +86 27 87199992

Abstract

HSV-2 spread is predominantly dependent on cell-to-cell contact. However, the underlying mechanisms remain to be determined. Here we demonstrate that HSV-2 gJ, which was previously assigned no specific function, promotes HSV-2 cell-to-cell spread and syncytia formation. In the context of viral infection, knockout or knockdown of gJ impairs HSV-2 cell-to-cell spread among epithelial cells or from epithelial cells to neuronal cells, which leads to decreased virus production, whereas ectopic expression of gJ enhances virus production. Mechanistically, gJ increases the expression levels of HSV-2 proteins, and also enhances viral protein expression and replication of heterologous viruses like HIV-1 and JEV, suggesting that HSV-2 gJ likely functions as a regulator of viral protein expression and virus production. Findings in this study provide a basis for further understanding the role of gJ in HSV-2 replication.

Keywords: HSV-2; gJ; cell-to-cell spread; protein expression; virus production

Introduction

HSV-2, a typical member of the α-herpesvirus subfamily, can infect the epithelium to cause genital herpes, establish latency in peripheral nervous system and be transmitted to the central nervous system, leading to a life-long latent infection (RC., 2001). HSV-2 infection also increases the risk of HIV-1 acquisition and transmission (Baeten et al., 2004; Freeman et al., 2006). The outermost envelope of HSV-2 virion contains at least 12 envelope glycoproteins which play important roles during the process of viral entry/egress and cell-to-cell spread (Haarr and Skulstad, 1994). In addition to viral essential proteins, the functions of many non-essential proteins of HSV-1/HSV-2 which are dispensable for virus replication (Baines and Roizman, 1991; Balan et al., 1994) have been revealed gradually. For example, the complex of gE and gI of HSV-1 acts as a receptor for immunoglobulin G (IgG) (Bell et al., 1990; Hanke et al., 1990; Johnson et al., 1988), facilitates efficient neuron-to-neuron transmission through synaptically linked neuronal pathways (Dingwell et al., 1995), and promotes cell-to-cell spread in vivo and across junctions of cultured cells (Dingwell et al., 1994). As the first viral chemokine-binding protein described, secreted HSV-1/HSV-2 gG has been shown to enhance chemokine function through modulation of receptor trafficking and oligomerization, to mediate the interaction between HSV-1/HSV-2 particles and a specific set of human chemokines (Martinez-Martin et al., 2016; Martinez-Martin et al., 2015; Viejo-Borbolla et al., 2012), and to modify NGF-TrkA signaling to attract free nerve endings to the site of infection (Cabrera et al., 2015). HSV-1 gM potently restricts HIV-1 by preventing intracellular transport and processing of Env gp160 (Polpitiya Arachchige et al., 2018) and partners with gN to modulate the viral fusion machinery (El Kasmi and

Lippe, 2015). Furthermore, HSV-1 gM and the gK/pUL20 complex have been shown to be important for the localization of gD and gH/L to viral assembly sites (Lau and Crump, 2015).

The documented new functions of these previously thought nonessential proteins are constantly refreshing our cognizance of HSV-1/HSV-2 and may have important implications for the rational design of potent antiviral strategies. HSV-2 gJ is a 92-amino acid late gene product encoded by the US5 open reading frame (ORF) (2), and so far has been assigned no specific function. Its orthologs HSV-1 gJ was thought to be a nonessential protein, and later found to inhibit apoptosis (22-25) and induce the formation of reactive oxygen species (26). Given that the aligned pairs of protein-coding regions for all genes (except US4, which in HSV-1 is grossly truncated) are around 83% sequence identity between HSV-1 and HSV-2 (Davison, 2011; Dolan et al., 1998), it is speculated that HSV-2 gJ may have a similar function as HSV-1 gJ.

In this study, we investigated the function of HSV-2 gJ in the context of viral infection. Our results indicate that HSV-2 gJ knockout or knockdown impairs plaque and syncytia formation which leads to decreased virus production, while ectopic expression of gJ enhances virus production. Furthermore, gJ increases the expression levels of other HSV-2 proteins and also enhances viral protein expression and replication of heterologous viruses like HIV-1 and JEV. Although we cannot rule out other possible mechanisms, our data together indicate that HSV-2 gJ likely functions as a regulator of viral protein expression. This is the first time that HSV-2 gJ has been shown to increase

viral protein expression and virus production, which consequently promotes HSV-2 cell-to-cell spread and syncytia formation.

Materials and Methods

Ethic statement

All protocols involving human subjects were reviewed and approved by the Local Research Ethics Committee. Informed written consents from the human subjects were obtained in this study.

Antibodies, plasmids and shRNAs

Mouse monoclonal antibody against FLAG was purchased from Sigma (F1804). Mouse monoclonal antibody against β-actin (sc-81178), rabbit polyclonal antibody against GFP (sc-8334), mouse monoclonal antibody against HSV-2 gD (sc-58154) were obtained from Santa Cruz. Mouse monoclonal antibody against HSV-2 gG (SAB4700764) was purchased from Sigma. Sheep polyclonal antibody against HSV-2 (PAB13979) was purchased from Abnova. Mouse monoclonal antibody against HSV-1+HSV-2 gB (ab6506) was purchased from Abcam.

The ORF of gJ with flag tag fused to the C-terminal was cloned into pcDNA3.1(+) (named pgJ-flag). The ORFs of immediate early proteins ICP0, ICP22 and ICP27 with flag tag fused to the C-terminal were cloned into pcDNA3.1(+), named pICP0-flag, pICP22-flag and pICP27-flag, respectively. The ORF of glycoproteins gB and gL with flag tag were cloned into pcDNA3.1(+) (named pgB and pgL-flag, respectively). All constructs were verified by DNA sequencing (Sunny Biotechnology Co. Ltd, Shanghai, China).

HSV-2 gJ shRNA and control shRNA were purchased from GENEWIZ. Lentiviral vector pLL3.7 was constructed to expresses gJ shRNA or control shRNA under the mouse U6 promoter. A CMV-EGFP reporter cassette was included in the vector to monitor expression.

Cell lines and viruses

African green monkey kidney cell line Vero, human cervical epithelial cell line HeLa and embryonic kidney cell line 293T were grown in Dulbecco's modified Eagle's medium (DMEM, Gibco) containing 10 % fetal bovine serum (FBS), 100 Units/ml penicillin and 100 Units/ml streptomycin at 37 °C in 5 % CO_2. Human retinal pigment epithelial cell line ARPE-19 was grown in DMEM/F-12 medium (50:50) supplemented with 10 % FBS, 100 Units/ml penicillin and 100 Units/ml streptomycin at 37 °C in 5 % CO_2. Human neuroblastoma cell line SH-SY5Y was grown in MEM supplemented with 10 % FBS, 100 Units/ml penicillin and 100 Units/ml streptomycin at 37 °C in 5 % CO_2. For the differentiation of SH-SY5Y cells, retinoic acid (RA, Sigma-Aldrich) was added at a final concentration of 10 μM in MEM supplemented with 10% FBS and maintained for 3 days.

The VgJ2, HgJ2, AgJ2 and SHgJ2 cell lines were generated by transfection of Vero, HeLa, ARPE-19 and SH-SY5Y cells, respectively, with a plasmid expressing flag-tagged HSV-2 gJ under the control of the viral thymidine kinase promoter. Transformed cells were selected for the ability to grow in the presence of geneticin and the expression of gJ-flag. The transfected cell lines were validated periodically to ensure the maintenance of gJ. VgJ2 and HgJ2 cells were passaged in DMEM supplemented with 10% FBS and 1 mg/ml

geneticin. AgJ2 cells were passaged in DMEM/F-12 medium (50:50) supplemented with 10% FBS and 500 ug/ml geneticin. SHgJ2 cells were passaged in MEM supplemented with 10% FBS and 500 ug/ml geneticin.

HSV-2 (strain G) was obtained from LGC standards. WT HSV-2-GFP carrying the complete genome of HSV-2 and green fluorescent protein (GFP) was kindly provided by Dr. Yasushi Kawaguchi, University of Tokyo, Japan, and served as the parental strain for construction of the gJ deleted virus. All viruses were grown and titered on Vero cells. Virus stock was stored at −80 °C before used for infection. The JEV strain SA14-14 was propagated in BHK-21 cells with DMEM containing 2% FBS. Virus titer was determined by a plaque assay on BHK-21 cells.

Isolation of human primary epithelial cells

Human foreskin tissues were obtained from Wuhan Children's Hospital (Wuhan Maternal and Child Healthcare Hospital), Tongji Medical College, Huazhong University of Science & Technology. Firstly, tissues were washed twice with PBS. The unusable tissues were dissected off and the remaining tissues were minced into 3 to 4 mm pieces with a sterile scissors. Thereafter, the tissue pieces were digested with Dispase for 10-12 h at 4°C and Dispase was removed. The container with the tissue pieces was placed on ice. After the discard of any remaining supernatant, 0.25% trypsin (1 ml of trypsin for every 100 mg of tissue) was added followed by incubation at 4°C for 6 to 8 h to maximize penetration of the enzyme. The tissue pieces with residual trypsin were shifted to 37°C and slightly shaked for 20 min. Warm complete medium was subsequently added to the tissue pieces

and gently dispersed by pipetting. The separated cells were filtered through a stainless steel strainer (0.5-1.0 mm) and cultured in complete medium for 3 h. Human primary epithelial cells were cultured in 12-well plates to 90-95% confluence before use.

Construction of gJ-null HSV-2

The Escherichia coli strain harboring the full-length HSV-2 BAC with GFP tag was the parental strain for the mutant virus gJ-null HSV-2 (named DelgJ HSV-2-GFP) was grown at 32°C in LB with 25μg/ml chloramphenicol. DelgJ HSV-2-GFP mutant was constructed via homologous recombination as previously described (Zhang et al., 2015). Briefly, Gel-purified PCR product was obtained using Kanamycin (Kan) primers with 50bp extension homologous to the gJ sequence. Thereafter, 5μg of PCR products was electroporated into 50μl competent DY380 cells containing HSV-2 BAC with GFP tag, with the settings of 1.8 kv (0.1cm cuvettes), 25μF, and 200Ω. Single colony were isolated and cultured to produce DelgJ HSV-2-GFP BAC plasmid. The DelgJ HSV-2-GFP mutant was confirmed by PCR detection and verified by DNA sequencing (Sangon Biotech, China). WT HSV-2-GFP and DelgJ HSV-2-GFP BAC plasmids were transfected into Vero cells to produce WT (WT HSV-2-GFP) and mutant viruses (DelgJ HSV-2-GFP), respectively. VgJ2 cells were infected with DelgJ HSV-2-GFP to produce the pseudovirus RgJ HSV-2-GFP. The existence of gJ in RgJ HSV-2-GFP virions was confirmed by Western blot (Fig S3).

Electron microscopy

Vero cells were infected with DelgJ HSV-2-GFP or WT HSV-2-GFP at an MOI of 5. At

24 hpi, cells were harvested and fixed with 2.5% glutaraldehyde/1% paraformaldehyde in cacodylate buffer (0.1M sodium cacodylate [pH 7.4], 35mM sucrose, 4mM $CaCl_2$), followed by staining in 1% OsO_4 and 4% uranyl acetate for 2 h and dehydrating in a graded ethanol series (50%–100%), and subsequently embedded in epoxy resin Embed-812 (Electron Microscopy Sciences). Thin sections (80 nm) were stained with 2% saturated uranyl acetate for 15 min, rinsed with water, and then stained with Reynolds' lead citrate for 15 min. Electron micrographs were taken on a Tecnai transmission electron microscope (FEI Tecnai G^2 20 TWIN) at an accelerating voltage of 200 kV.

One-step growth curve

One-step growth curve was measured following infection of preformed Vero, HeLa, or ARPE-19 monolayers with HSV-2 at an MOI of 10 PFU/cell. Adsorption was allowed to proceed for 2 h at 37 °C before the inoculum was removed and residual inoculum was neutralized by incubation for 15 min with medium containing the HSV-2 pAb (1:100 dilution). The Vero, HeLa, or ARPE-19 monolayers were then washed twice with fresh medium and incubated for 0, 6, 12, 18 and 24 hours post infection (hpi) before being harvested and assayed for virus yields.

Infectious center assay

Infectious center assay was carried out as previously described (Jenssen et al., 2008). In brief, Vero or HeLa cells plated in 6-well plates at 50% confluence were exposed to DelgJ HSV-2-GFP or WT HSV-2-GFP at an MOI of 5 PFU/cell at 37°C. In parallel, VgJ2 or HgJ2 cells were infected with RgJ HSV-2-GFP. After 2 h of incubation, cells were

washed once with PBS and then treated with proteinase K for 45 min to remove adsorbed but not internalized viruses. Proteinase K was then inactivated with 2 mM PMSF in PBS containing 3% bovine seroalbumin (BSA). The monolayer was then washed twice with PBS and cultured in growth medium supplemented with an anti-HSV-2 antibody (PAB13979, Abnova) at a dilution of 1:1000 to neutralize the extracellular HSV-2. After a total incubation of 5.5 h, the infected cells were detached with trypsin-EDTA, resuspended in growth medium, and ~80 cells were plated onto 50% confluent monolayers of uninfected Vero, HeLa, VgJ2 or HgJ2 cells. Cells were maintained in growth medium containing anti-HSV-2 polyclonal antibody. 2 days later, cells were fixed and nuclei were dyed by Hoechst 33342 (Beyotime). Stained cells were analyzed using confocal microscopy (NIKON). Plaques and syncytia formation were photographed and the plaque areas were compared.

Flow cytometry

For cell-to-cell spread assay, HeLa or ARPE-19 cells were infected with the same amount of DelgJ HSV-2-GFP and WT HSV-2-GFP, respectively, at an MOI of 10 for 2h. In parallel, HgJ2 or AgJ2 cells were infected with RgJ HSV-2-GFP. After digestion by trypsin, 100 cells per samples were taken out followed by co-cultivation with HeLa, ARPE-19, HgJ2, AgJ2, SHgJ2 or SH-SY5Y cells which were labeled with CellTracker Blue fluorescence dye. 2 days later, cells were washed three times with flow cytometry buffer and fixed with 1% paraformaldehyde. The CellTracker Blue^{+} GFP^{+} populations were analyzed using FACS Calibur flow cytometer (BD). Data were analyzed by Flowjo software.

Viral adsorption and entry assay

HeLa or ARPE-19 cells (~8×10^5 per well) were plated onto 6-well plates overnight. To assess the adsorption of DelgJ HSV-2-GFP or WT HSV-2-GFP, the cultures were subsequently replaced with cold (4°C) medium and placed on ice for 10 min, followed by the addition of precooled DelgJ HSV-2-GFP or WT HSV-2-GFP (MOI=5 PFU/cell) and an incubation at 4°C for 60 min. After removal of viruses, cells were washed three times with cold PBS and harvested. The HSV-2 genomic DNA was exacted using QIAamp DNA Blood Mini Kit (51104, Qiagen) and then detected by quantitative PCR. To assess the entry of DelgJ HSV-2-GFP or WT HSV-2-GFP, the cultures were subsequently infected with DelgJ HSV-2-GFP or WT HSV-2-GFP (MOI=5 PFU/cell) and incubated at 37°C for 2h. After removal of viruses, the monolayers were treated with proteinase K for 45 min to remove adsorbed but not internalized viruses. Proteinase K was then inactivated with 2 mM PMSF in PBS containing 3% BSA followed by two washes with PBS. Cells were harvested and the HSV-2 genomic DNA was extracted using QIAamp DNA Blood Mini Kit (51104, Qiagen). The copies of HSV-2 genomic DNA were detected by quantitative PCR.

Quantitative PCR

HeLa, ARPE-19 or SH-SY5Y cells were infected with DelgJ-HSV-2-GFP or WT-HSV-2-GFP at an MOI of 5 PFU/cell or mock infected. In parallel, HgJ2, AgJ2 or SHgJ2 cells were infected with RgJ HSV-2-GFP. At 48 hpi, cells were collected and the

viral genomic DNA was extracted using QIAamp DNA Blood Mini Kit (51104, Qiagen). The genomic DNAs obtained from HeLa, ARPE-19 or SH-SY5Y cells infected with DelgJ-HSV-2-GFP or WT-HSV-2-GFP or mock infected, or from HgJ2, AgJ2 or SHgJ2 cells infected with RgJ HSV-2-GFP were used as the templates for the amplification of a highly specific nucleotide region of ICP0 gene (RL2). Primers 5′-GTGCATGAAGACCTGGATTCC -3′ and 5′- GGTCACGCCCACTATCAGGTA -3′ were used for ICP0 amplification (Cheshenko et al., 2010). GAPDH was used as an internal control amplified with primers 5'-GGGAAGCTCACTGGCATGG-3' and 5'-TTACTCCTTGGAGGCCATGT-3'. Relative quantitative PCR was performed using a SYBR Green Real-Time PCR Master Mix (Toyobo) Dye and an ABI StepOne real-time PCR system (Applied Biosystems). The final reaction conditions were as follow: 95°C for 1 min, followed by 40 cycles of 95°C for 15 sec, 60°C for 15 sec, and 72°C for 45 sec. The difference in gene expression was calculated on the basis of $2^{-\Delta\Delta CT}$ values.

Production and quantitation of HIV-1

293T cells were transfected with plasmid pNL4-3 and pgJ-flag, pgL-flag or pcDNA3.1 using Lipofectamine 2000 (Invitrogen) according to the manufacturer's instructions to produce HIV-1. At 48h post transfection, supernatants and cells were harvested separately. The expression level of p24 in supernatants or cell lysates was measured by p24 ELISA. The titer of infectious HIV-1 in supernatants was analyzed in an infection assay using supernatants containing HIV-1 to infect TZM-bl cells.

Western Blot

Prepared cell lysates or immunoprecipitates were resolved by 10% or 12% SDS-PAGE and transferred to 0.45 μm polyvinylidene difluoride membranes (Millipore). Nonspecific binding was blocked using 5% non-fat milk in PBS overnight at 4°C. The membrane was incubated with primary antibody against gB at a dilution of 1:2000, gD at a dilution of 1:1000, FLAG at a dilution of 1:3000, GFP at a dilution of 1:1000 and β-actin at a dilution of 1:500, for 1 h at 37°C. The membrane was washed five times with 0.1% Tween 20/PBS, followed by incubation for 1 h with HRP conjugated goat anti–rabbit secondary antibody (1:10,000, BA1054, Boster) or HRP conjugated goat anti–mouse secondary antibody (1:10,000, BA1050, Boster). After five washes with 0.1% Tween-20/PBS, the bands were visualized by exposure to FluorChem HD2 Imaging System (Alpha Innotech) after the addition of chemiluminescent substrate (SuperSignal® West Dura Extended Duration Substrate, 34075, Thermo Scientific Pierce).

Statistical analysis

All experiments were repeated for at least three times. Data are presented as mean ± standard deviation (SD) unless otherwise specified. All statistical analysis was performed by GraphPad Prism. The difference of mean value was analyzed by a paired Student's t-test. $P < 0.05$ was considered statistically significant.

Results

Virus production is impaired in cells infected with gJ-null HSV-2

To investigate the function of HSV-2 gJ during viral infection, Bacterial artificial chromosome (BAC) plasmid containing the gJ deleted HSV-2 genome with GFP tag was constructed. The BAC DNA plasmids were transfected into Vero cells to produce gJ-null HSV-2 (named DelgJ HSV-2-GFP) and wild-type HSV-2 (WT HSV-2-GFP), respectively. The ORFs of gJ and Kanamycin (Kan) in DelgJ HSV-2-GFP and WT HSV-2-GFP were confirmed by PCR (Fig. S1 A). The fluorescence of GFP was detected in Vero cells infected with the four DelgJ HSV-2-GFP clones or WT HSV-2-GFP (Fig. S1 B). Electron microscopy also demonstrated the production of virions in Vero cells infected with the four DelgJ HSV-2-GFP clones and WT HSV-2-GFP, respectively (Fig. S1 C). Since US4 (coding gG) locates in the upstream of US5 (coding gJ), and US5 and US6 (coding gD) form a transcribed gene cluster (Dolan et al., 1998), Western blot analysis was conducted to confirm that gJ ORF deletion did not affect the expression of its adjacent gene (US4 and US6) (Fig. S1 D). These results indicated that the constructed gJ deleted HSV-2 was successfully produced in Vero cells. The four DelgJ HSV-2-GFP clones and WT HSV-2-GFP were used to infect Vero cells at an MOI of 5 PFU/cell. The supernatants and cells were collected to measure virus yields by plaque assay at 24 hpi. As shown in Fig. S2, the viral yields of the four DelgJ HSV-2-GFP clones were ~2 fold less than that of WT HSV-2-GFP. Given that the four DelgJ HSV-2-GFP clones had a similar impact on virus production, the 4# DelgJ HSV-2-GFP was used for subsequent experiments.

The rates of adsorption and entry of DelgJ HSV-2-GFP and WT HSV-2-GFP were

compared in HeLa and ARPE-19 cell monolayers. To assess the adsorption, the HeLa and ARPE-19 cultures were subsequently replaced with cold (4°C) medium and placed on ice for 10 min, followed by the addition of precooled DelgJ HSV-2-GFP or WT HSV-2-GFP (MOI=5 PFU/cell) and an incubation at 4°C for 60 min. After removal of viruses, infected cells were collected and the viral genomic DNA were extracted and analyzed by monitoring the HSV-2 IE protein ICP0 using relative quantitative PCR. As shown in Fig. 1A, the mean fold change of ICP0 was around one, indicating that there was no difference in adsorption between DelgJ HSV-2-GFP and WT HSV-2-GFP. To assess the entry, the HeLa and ARPE-19 cultures were subsequently infected with DelgJ HSV-2-GFP or WT HSV-2-GFP (MOI=5 PFU/cell) and incubated at 37°C for 2h. After removal of viruses, the monolayers were treated with proteinase K to remove adsorbed but not internalized viruses. Cells were subsequently harvested and the HSV-2 genomic DNA was extracted. The copies of HSV-2 genomic DNA were compared by relative quantitative PCR. The entry rates of mutant and wild-type HSV-2 were also similar (Fig. 1B). The virus production was subsequently examined. DelgJ HSV-2-GFP and WT HSV-2-GFP were used to infect Vero, ARPE-19, HeLa, and SH-SY5Y cells at an MOI of 5 PFU/cell. At 24 hpi, the supernatants and cells were collected and the virus yields were measured by plaque assay. As shown in Fig. 1C, the viral yield of DelgJ HSV-2-GFP was 2-3 fold less than that of WT HSV-2-GFP in the four different types of cell lines. The paralleled infected cells were collected and the viral genomic DNA was analyzed by monitoring the HSV-2 IE protein ICP0 with relative quantitative PCR. The mean fold change of ICP0 in DelgJ HSV-2-GFP-infected cells was similar to that in WT HSV-2-GFP-infected cells, indicating that the virus production of DelgJ HSV-2-GFP was

much less than that of WT HSV-2-GFP (Fig. 1D). Following harvest of cell lysates at 24 hpi, the expression level of viral protein gD in DelgJ HSV-2-GFP or WT HSV-2-GFP infected cells were determined by western blot. As shown in Fig. 1E, the expression level of gD in WT HSV-2-GFP infected cells was higher than that from DelgJ HSV-2-GFP infected cells.

We also examined the virus production of WT HSV-2 and DelgJ HSV-2 in human primary epithelial cells isolated from human foreskin tissues. The results of primary epithelial cells isolated from 5 donors were similar to those from the epithelial cell lines (Fig. 1F). One-step growth curve was measured following infection of preformed Vero monolayers. Although similar growth curves were achieved, the virus production of DelgJ HSV-2-GFP was ~2 fold less than that of WT HSV-2-GFP at 18 and 24hpi (Fig. 2). These data together demonstrated that HSV-2 gJ is beneficial for virus production.

Knockdown of gJ by shRNA decreases HSV-2 replication

The above results were obtained from the constructed recombinant viruses DelgJ HSV-2-GFP and WT HSV-2-GFP containing GFP in their genomes. To further confirm these findings, we assessed the replication of wild-type HSV-2 strain G by shRNA knockdown of gJ. Serial concentration gradients of retroviral vectors expressing gJ shRNA or control shRNA were generated and transfected into HeLa cells pre-transfected with pgJ-flag or pcDNA3.1. Western blot showed that, at 48 hours post transfection, all of the three gJ shRNAs reduced the expression of gJ with different efficiency with the #1 gJ shRNA (Fig. 3A) being the most effective one, and the #1 gJ shRNA was therefore used

in the following experiments. HeLa and ARPE-19 cells were transfected with retroviral vectors expressing #1 gJ shRNA or control shRNA followed by infection with HSV-2 strain G at an MOI of 5 PFU/cell. Supernatants and cells were collected at 24 hpi, and thereafter, the viral yield of samples was analyzed using plaque assays. As shown in Fig. 3B, the virus production of HSV-2 decreased 2-3 fold in both HeLa and ARPE-19 cells treated with gJ shRNA, confirming that gJ is indeed important for HSV-2 production.

Ectopic expression of gJ enhances the replication of both wild-type and gJ-null HSV-2

Having demonstrated that both gJ knockout and knockdown resulted in decreased HSV-2 production, we next asked whether ectopic expression of gJ has an impact on HSV-2 replication. For this purpose, HeLa and ARPE-19 cells were transfected with pgJ-flag or pcDNA3.1 followed by infection with WT HSV-2-GFP or DelgJ HSV-2-GFP at an MOI of 5 PFU/cell. Supernatants and cells were collected at 24 hpi, and thereafter, the viral yield was analyzed by plaque assays. As shown in Fig. 4A and C, the virus production of both WT HSV-2-GFP and DelgJ HSV-2-GFP was increased in the gJ-expressing cells. The expression of HSV-2 protein gD in the parallel samples was also measured by Western blot, showing that the expression level of gD in WT HSV-2-GFP infected cells was higher than that in DelgJ HSV-2-GFP infected cells (Fig. 4B and D). Taken together, these results suggested that gJ appears not to be essential for HSV-2 replication and transmission and instead may function as a regulatory protein to increase virus production.

Knockout of HSV-2 gJ significantly impaired plaque and syncytia formation and decreased virus production

We observed that all the cells infected with DelgJ HSV-2-GFP or WT HSV-2-GFP turned round and there was no obvious difference between the pathological cells (data not shown) infected with a high MOI of the viruses (great than or equal to 5). On the contrary, most of the pathological cells infected with WT-HSV-2-GFP were larger than those infected with DelgJ HSV-2-GFP when Vero cells were infected at a lower MOI (~0.1) (Fig. S1B). It seemed that the syncytia formation decreased in cells infected with the DelgJ HSV-2-GFP. We further investigated the impact of HSV-2 gJ on plaque and syncytia formation using a Vero cell line stably expressing gJ-flag (VgJ2). VgJ2 cells were infected with DelgJ HSV-2-GFP at an MOI of 1 PFU/cell to produce the pseudovirus RgJ HSV-2-GFP. At 24hpi, pseudoviruses were harvested and concentrated through ultracentrifugation. Following Western blot, the expression of gB and gJ-flag was confirmed in the lysates containing DelgJ HSV-2-GFP or RgJ HSV-2-GFP (Fig. S3). To achieve a better observation, DelgJ HSV-2-GFP and WT HSV-2-GFP were used to infect Vero and HeLa cells at an extremely low MOI (~80 PFU/1×10^6 cells), respectively. After removal of the inoculum, cells were maintained in growth medium containing an anti-HSV-2 antibody (Abnova) to neutralize extracellular HSV-2. Plaques and syncytia formation were photographed and the plaque areas were compared after 48 h incubation at 37°C. In parallel, we examined the plaque formation of RgJ HSV-2-GFP in VgJ2 cells. As shown in Fig. 5A and B, DelgJ HSV-2-GFP produced significantly smaller plaques on Vero monolayers than did WT HSV-2-GFP, but produced full-size plaques on VgJ2 cells. A HeLa cell line stably expressing gJ-flag (HgJ2) was also examined. Fluorescence

microscopy analysis of plaque and syncytia formation also showed that, compared with those of WT HSV-2-GFP, plaques were smaller and syncytia formation was significantly inhibited in Vero and HeLa cells infected with DelgJ HSV-2-GFP, whereas full-size plaques were observed on VgJ2 or HgJ2 cells infected with RgJ HSV-2-GFP (Fig. 5C). Meanwhile, an ARPE-19 cell line stably expressing gJ-flag (AgJ2) was also tested. HeLa or ARPE-19 cells were infected with DelgJ HSV-2-GFP or WT HSV-2-GFP at a very low MOI (~80 PFU/1×10^6 cells). In parallel, HgJ2 or AgJ2 cells were infected with RgJ HSV-2-GFP. After 48 h incubation at 37°C, cells were harvested and analyzed by flow cytometry. As shown in Fig. 6A, in both HeLa and ARPE-19 cells, the proportion of GFP^+ cells infected with DelgJ HSV-2-GFP was less than that with WT HSV-2-GFP, while the proportion of GFP^+ cells infected with RgJ DelgJ HSV-2 was similar to that with WT HSV-2-GFP, suggesting that cell-to-cell spread of DelgJ HSV-2-GFP was indeed slower than that of WT HSV-2-GFP in monolayers, though gJ did not impact the absorption and entry of virus particles (Fig. 1A and 1B).

To determine whether gJ influences the neuron-to-neuron transmission of HSV-2, the differentiated neuron-like cells SH-SY5Y were infected with DelgJ HSV-2-GFP or WT HSV-2-GFP at a very low MOI (~80 PFU/1×10^6 cells) followed by analysis with flow cytometry. A SH-SY5Y cell line stably expressing gJ-flag (SHgJ2) was also examined. In parallel, SHgJ2 cells were infected with RgJ HSV-2-GFP. As shown in Fig 6A, the results obtained from SH-SY5Y cells were in accordance with those from epithelia cells HeLa and ARPE-19 (Fig. 6A). In parallel, the levels of viral genomic DNA and virus production were also examined. Relative quantitative PCR and plaque assay showed that

the viral genomic DNA and the viral yield in cells infected with DelgJ HSV-2-GFP were less than those with WT HSV-2-GFP or RgJ HSV-2-GFP (Fig. 6B and C). These results indicated that knockout of gJ significantly impacted HSV-2 cell-to-cell spread and contributed to the decreased virus production.

gJ promotes cell-to-cell spread of HSV-2 among epithelial cells or from epithelial cells to neuronal cells

HSV-2 spread is predominantly dependent on cell-to-cell contact rather than on particle release and reentry (RC., 2001). The inhibition of virus plaque and syncytia formation in DelgJ-HSV-2-GFP infected cell monolayers indicated that gJ is important for an efficient cell-to-cell spread of the virus. To elucidate whether gJ-promoted cell-to-cell spread is cell type specific, we conducted experiments to determine the ratio of HSV-2 being transferred from infected to uninfected cells. Firstly, HeLa or ARPE-19 cells were infected with the same amount of DelgJ HSV-2-GFP or WT HSV-2-GFP at an MOI of 10 for 2h. In parallel, HgJ2 or AgJ2 cells were infected with RgJ HSV-2-GFP. Following digestion by trypsin, 100 cells per samples were co-cultivated with corresponding HeLa, ARPE-19, HgJ2 or AgJ2 cells labeled with CellTracker Blue fluorescence dye for 2 days. HSV-2 transmission from infected to uninfected cells was subsequently quantified by analyzing CellTracker Blue^{+} GFP^{+} populations with flow cytometry. As shown in Fig. 7B and E, the proportion of CellTracker Blue^{+} GFP^{+} HeLa or ARPE-19 cells in sample containing DelgJ-HSV-2-GFP was 0.199 ± 0.041% and 0.201 ± 0.044% respectively, while the proportion of CellTracker Blue^{+} GFP^{+} HeLa or ARPE-19 cells in sample containing WT HSV-2-GFP was 0.680 ± 0.096% and 0.857 ± 0.051%, respectively. As

expected, the proportion of CellTracker Blue$^+$ GFP$^+$ cells increased to 0.654 ± 0.094% and 0.846 ± 0.053% in HgJ2 and AgJ2, respectively. Virus production of the parallel samples was also detected by plaque assay. The viral yield from DelgJ HSV-2-GFP infected cells was less than that from WT HSV-2-GFP infected cells or RgJ HSV-2-GFP (Fig. 7C and F). These results together informed that cell-to-cell spread of HSV-2 promoted by gJ from HeLa to HeLa cells was similar to that from ARPE-19 to ARPE-19 cells, indicating that gJ can promote HSV-2 cell-to-cell spread among epithelial cells.

In addition to mucosal epithelial cells, it has been documented that HSV-1/HSV-2 can infect sensory neurons following primary infections of mucosal and submucosal tissues (Cook and Stevens, 1973; Kristensson et al., 1971). To determine whether gJ plays a role in HSV-2 epithelial cell-to-neuronal cell transmission, epithelial cells ARPE-19 and the differentiated neuron-like cells SH-SY5Y were used for subsequent experiments. ARPE-19 cells were infected with the same amount of DelgJ HSV-2-GFP or WT HSV-2-GFP at an MOI of 10 for 2h, followed by digestion with trypsin. In parallel, AgJ2 cells were infected with RgJ HSV-2-GFP. 100 cells per samples were co-cultivated with uninfected SH-SY5Y or SHgJ2 cells labeled with CellTracker Blue fluorescence dye for 2 days. The CellTracker Blue$^+$ GFP$^+$ populations were analyzed by flow cytometry, while the virus production of the parallel samples was detected by plaque assay. As shown in Fig. 7H, the proportion of CellTracker Blue$^+$ GFP$^+$ SH-SY5Y cells in sample containing DelgJ HSV-2-GFP was 0.154 ± 0.053%, while the proportion of CellTracker Blue$^+$ GFP$^+$ ARPE-19 cells in samples containing WT HSV-2-GFP and RgJ HSV-2-GFP was 0.853 ± 0.109% and 0.891 ± 0.096%, respectively, indicating that the proportion of newly

infected cells which co-cultured with DelgJ HSV-2-infected cells was fewer than that with WT or RgJ HSV-2-infected cells and that the cell-to-cell spread of DelgJ HSV-2 was slower than that of WT or RgJ HSV-2. In agreement, the viral yield of samples containing DelgJ HSV-2-GFP was less than that of samples containing WT HSV-2-GFP or RgJ HSV-2-GFP (Fig. 7I). These data highlighted that HSV-2 gJ can promote cell-to-cell spread of the virus between different cell types, and of particular interest from epithelial cells to neuronal cells.

HSV-2 gJ increases viral protein expression and virus production

Given that the expression level of viral protein gD in cells infected with WT HSV-2-GFP was higher than that with DelgJ HSV-2-GFP, we conducted experiments to address whether gJ alone influence the expression level of other HSV-2 proteins. 293T cells were contransfected with pcDNA3.1, pgL-flag or pgJ-flag together with plasmids expressing immediate early proteins ICP0, ICP22 or ICP27. Western blot showed that the expression level of the viral immediate early proteins in cells cotransfected with gJ-flag plasmid was substantially higher than that with pcDNA3.1 or pgL-flag (Fig. 8A left). We also assessed the expression level of the late protein gB, which is crucial for cell-to-cell spread of the virus. 293T cells were contransfected with pcDNA3.1, pgL-flag or pgJ-flag together with plasmid expressing gB. Western blot showed that the expression level of gB increased in gJ-flag transfected cells (Fig. 8A right). The correlation between the dose of gJ and the expression level of ICP27 was further examined. As shown in Fig. 8B, the increase of gJ-flag dose positively correlated with a higher expression level of ICP27. A positive association between the expression of gJ and other HSV-2 viral proteins indicated that gJ

can increase the expression of HSV-2 viral proteins.

It was previously reported that HSV-1 ICP0 and ICP4 stimulated HIV-1 replication when cotransfected with an infectious HIV-1 clone (Ostrove et al., 1987). In addition, US11 protein was also shown to increase HIV-1 expression (Diaz et al., 1996). We asked whether gJ can increase viral protein expression and virus yield of other viruses. 293T cells were cotransfected with pcDNA3.1, pgL-flag or pgJ-flag together with an infectious HIV-1 clone (pNL4-3). At 48h post transfection, supernatants and cells were harvested. The expression level of p24 in supernatants and cell lysates was measured by ELISA, while the production of infectious HIV-1 in supernatants was analyzed by using supernatants containing HIV-1 to infect TZM-bl cells. As shown in Fig. 8C, in both supernatants and cell lysates, the expression level of p24 in gJ-expressing cells was significantly higher than that in gL-flag or pcDNA3.1-transfected cells. Accordingly, the infectious HIV-1 produced from gJ-expressing cells was much more than that from gL-flag or pcDNA3.1-transfected cells (Fig. 8D). We also examined the effect of HSV-2 gJ on a flavivirus JEV. 293T cells were contransfected with pcDNA3.1, pgL-falg or pgJ-flag together with the plasmid expressing JEV NS3. Western blot showed that the expression level of NS3 in gJ-expressing cells was higher than that in gL-flag or pcDNA3.1-transfected cells (Fig. 8E). To assess the influence of gJ on virus production, HeLa cells transfected with control pcDNA3.1 or plasmid expressing gJ-flag or gL-flag were infected with JEV at an MOI of 10 PFU/cell. At 24hpi, the viral yield was measured by plaque assay. Compared to that in pcDNA3.1-transfected cells, the production of JEV in gJ-expressing cells increased ~2.5-fold (Fig. 8F). Collectively, these results suggested

that HSV-2 gJ can increase viral protein expression and virus production regardless of virus species.

Discussion

The major mode of HSV-2 transmission is cell-to-cell spread, an efficient strategy for the virus to circumvent the host immune response. However, despite being a predominant mode of viral spread in vivo, cell-to-cell transmission has not been studied to the same extent as virus-to-cell transmission. In this study, we found that, in the context of viral infection, HSV-2 gJ promotes cell-to-cell spread and syncytia formation. Moreover, gJ-promoted cell-to-cell spread of HSV-2 was observed not only among HeLa or ARPE-19 cells, but also from ARPE-19 to differentiated SH-SY5Y cells, suggesting that gJ likely facilitates cell-to-cell spread of HSV-2 among epithelial cells as well as from epithelial cells to neuronal cells. It is a hazardous voyage from the primary infection sites to the latent infection sites in vivo for the virus. To date, there has been no evidence that HSV-2 uses antigenic variation to escape host control, implying that the virus likely uses alternative strategies such as cell-to-cell spread in order to be successfully transmitted. Our findings that gJ facilitates cell-to-cell spread of the virus among epithelial cells and from epithelial cells to neuronal cells may have important implications when considering HSV-2 mucosal transmission as well as its dissemination cross different tissues in vivo.

To investigate the function of HSV-2 gJ during viral infection, we constructed a gJ-null HSV-2 (named DelgJ HSV-2-GFP) and made pseudovirus RgJ HSV-2-GFP using our constructed stable cell lines expressing gJ. The results demonstrated that the viral yields, plaque and syncytia formation were rescued on cell lines stably expressing gJ, suggesting that the non-essential protein, HSV-2 gJ, is likely to be beneficial for cell-to-cell spread and virus production. The difference of viral yields between gJ-null HSV-2 (DelgJ

HSV-2-GFP) and WT HSV-2 was relatively small (~2-3 fold) but statistically significant, suggesting that HSV-2 gJ is likely to be beneficial for virus production, although the biological significance remains to be addressed in future animal study.

Our gJ knockout and knockdown experiments together demonstrated that HSV-2 gJ is beneficial for viral protein expression and virus production, which consequently promotes HSV-2 cell-to-cell spread and syncytia formation. Major participants in the immune escape process include HSV-1/HSV-2 envelop proteins which were reported to be involved in cell-to-cell spread such as gB (Cheshenko and Herold, 2002) or membrane fusion (Lin et al., 2011). We demonstrated that gJ increases the expression levels of other HSV-2 proteins. Although beyond the scope of this current study, it will be interesting to address the precise mechanism by which HSV-2 gJ influences viral protein expression and virus production. It is probable that the expression level of proteins involved in cell-to-cell spread or membrane fusion is likely to be enhanced which further promotes cell-to-cell spread and syncytia formation. Since HSV-2 gJ increases the expression level of viral proteins and virus production, we hypothesized that gJ might also increase viral protein expression and virus yields of other virus species. Indeed, gJ not only enhanced the expression level of viral proteins including HIV-1 p24 and JEV NS3, but also increased the production of the tested viruses HIV-1 and JEV. Although we cannot rule out other possible mechanisms, our findings provide evidence that HSV-2 gJ likely functions as a regulator of viral protein expression and virus production.

It was thought that HSV-1 gJ is a nonessential glycoprotein dispensable for virus

replication in cultured cells as disruption of the US5 gene did not significantly alter HSV-1 virus virulence (Baines and Roizman, 1991; Balan et al., 1994). Nevertheless, several studies later reported that HSV-1 gJ plays roles in inhibiting apoptosis (22-25) and in inducing the formation of reactive oxygen species (26). In the current study, we have revealed a novel role of HSV-2 gJ, showing that gJ promotes cell-to-cell spread and syncytia formation, and likely functions as a regulator of viral protein expression and virus production. HSV-1 gJ was previously reported to inhibit apoptosis and has no impact on cell-to-cell spread (Baines and Roizman, 1991; Balan et al., 1994). The different roles played by HSV-2 and HSV-1 gJs in cell-to-cell spread may reflect the primary transmission modes of these two viruses. HSV-2 transmission is mainly through cell-to-cell contact whereas the major mode of HSV-1 transmission is via virus-to-cell infection.

Conclusions

In conclusion, we have demonstrate that HSV-2 gJ promotes HSV-2 cell-to-cell spread and syncytia formation, and further showed that gJ can increase viral protein expression and virus production.

Acknowledgements

This work was supported by the National Natural Science Foundation of China (31570165 and 81572009), the National Mega-Projects against Infectious Diseases (2018ZX10301406-002 and 2018ZX10301405-003), and the Open Research Fund Program of the State Key Laboratory of Virology of China (2017IOV006). We thank the Core Facility and Technical Support at Wuhan Institute of Virology for technique supports of Electronic Microscopy (Ms. Pei Zhang), Confocal Microscopy (Dr. Ding Gao) and Flow Cytometry (Ms. Juan Min).

References

Baeten, J.M., McClelland, R.S., Corey, L., Overbaugh, J., Lavreys, L., Richardson, B.A., Wald, A., Mandaliya, K., Bwayo, J.J., Kreiss, J.K., 2004. Vitamin A supplementation and genital shedding of herpes simplex virus among HIV-1-infected women: a randomized clinical trial. J Infect Dis 189, 1466-1471.

Baines, J.D., Roizman, B., 1991. The open reading frames UL3, UL4, UL10, and UL16 are dispensable for the replication of herpes simplex virus 1 in cell culture. J Virol 65, 938-944.

Balan, P., Davis-Poynter, N., Bell, S., Atkinson, H., Browne, H., Minson, T., 1994. An analysis of the in vitro and in vivo phenotypes of mutants of herpes simplex virus type 1 lacking glycoproteins gG, gE, gI or the putative gJ. J Gen Virol 75 (Pt 6), 1245-1258.

Bell, S., Cranage, M., Borysiewicz, L., Minson, T., 1990. Induction of immunoglobulin G Fc receptors by recombinant vaccinia viruses expressing glycoproteins E and I of herpes simplex virus type 1. J Virol 64, 2181-2186.

Cabrera, J.R., Viejo-Borbolla, A., Martinez-Martin, N., Blanco, S., Wandosell, F., Alcami, A., 2015. Secreted herpes simplex virus-2 glycoprotein G modifies NGF-TrkA signaling to attract free nerve endings to the site of infection. PLoS Pathog 11, e1004571.

Cheshenko, N., Herold, B.C., 2002. Glycoprotein B plays a predominant role in mediating herpes simplex virus type 2 attachment and is required for entry and cell-to-cell spread. J Gen Virol 83, 2247-2255.

Cheshenko, N., Trepanier, J.B., Segarra, T.J., Fuller, A.O., Herold, B.C., 2010. HSV usurps eukaryotic initiation factor 3 subunit M for viral protein translation: novel prevention target. PLoS One 5, e11829.

Cook, M.L., Stevens, J.G., 1973. Pathogenesis of herpetic neuritis and ganglionitis in mice: evidence for intra-axonal transport of infection. Infect Immun 7, 272-288.

Davison, A.J., 2011. Evolution of sexually transmitted and sexually transmissible human herpesviruses. Ann N Y Acad Sci 1230, E37-49.

Diaz, J.J., Dodon, M.D., Schaerer-Uthurralt, N., Simonin, D., Kindbeiter, K., Gazzolo, L., Madjar, J.J., 1996. Post-transcriptional transactivation of human retroviral envelope glycoprotein expression by herpes simplex virus Us11 protein. Nature 379, 273-277.

Dingwell, K.S., Brunetti, C.R., Hendricks, R.L., Tang, Q., Tang, M., Rainbow, A.J., Johnson, D.C., 1994. Herpes simplex virus glycoproteins E and I facilitate cell-to-cell spread in vivo and across junctions of cultured cells. J Virol 68, 834-845.

Dingwell, K.S., Doering, L.C., Johnson, D.C., 1995. Glycoproteins E and I facilitate neuron-to-neuron spread of herpes simplex virus. J Virol 69, 7087-7098.

Dolan, A., Jamieson, F.E., Cunningham, C., Barnett, B.C., McGeoch, D.J., 1998. The genome sequence of herpes simplex virus type 2. J Virol 72, 2010-2021.

El Kasmi, I., Lippe, R., 2015. Herpes simplex virus 1 gN partners with gM to modulate the viral fusion machinery. J Virol 89, 2313-2323.

Freeman, E.E., Weiss, H.A., Glynn, J.R., Cross, P.L., Whitworth, J.A., Hayes, R.J., 2006. Herpes simplex virus 2 infection increases HIV acquisition in men and women: systematic review and meta-analysis of longitudinal studies. AIDS 20, 73-83.

Haarr, L., Skulstad, S., 1994. The herpes simplex virus type 1 particle: structure and molecular functions. Review article. APMIS 102, 321-346.

Hanke, T., Graham, F.L., Lulitanond, V., Johnson, D.C., 1990. Herpes simplex virus IgG Fc receptors induced using recombinant adenovirus vectors expressing glycoproteins E and I. Virology 177, 437-444.

Jenssen, H., Sandvik, K., Andersen, J.H., Hancock, R.E., Gutteberg, T.J., 2008. Inhibition of HSV cell-to-cell spread by lactoferrin and lactoferricin. Antiviral Res 79, 192-198.

Johnson, D.C., Frame, M.C., Ligas, M.W., Cross, A.M., Stow, N.D., 1988. Herpes simplex virus immunoglobulin G Fc receptor activity depends on a complex of two viral glycoproteins, gE and gI. J Virol 62, 1347-1354.

Kristensson, K., Lycke, E., Sjostrand, J., 1971. Spread of herpes simplex virus in peripheral nerves. Acta Neuropathol 17, 44-53.

Lamers, S.L., Newman, R.M., Laeyendecker, O., Tobian, A.A., Colgrove, R.C., Ray, S.C., Koelle, D.M., Cohen, J., Knipe, D.M., Quinn, T.C., 2015. Global Diversity within and between Human Herpesvirus 1 and 2 Glycoproteins. J Virol 89, 8206-8218.

Lau, S.Y., Crump, C.M., 2015. HSV-1 gM and the gK/pUL20 complex are important for the localization of gD and gH/L to viral assembly sites. Viruses 7, 915-938.

Lin, L.T., Chen, T.Y., Chung, C.Y., Noyce, R.S., Grindley, T.B., McCormick, C., Lin, T.C., Wang, G.H., Lin, C.C., Richardson, C.D., 2011. Hydrolyzable tannins (chebulagic acid and punicalagin) target viral glycoprotein-glycosaminoglycan interactions to inhibit herpes simplex virus 1 entry and cell-to-cell spread. J Virol 85, 4386-4398.

Martinez-Martin, N., Viejo-Borbolla, A., Alcami, A., 2016. Herpes simplex virus particles interact with chemokines and enhance cell migration. J Gen Virol 97, 3007-3016.

Martinez-Martin, N., Viejo-Borbolla, A., Martin, R., Blanco, S., Benovic, J.L., Thelen, M., Alcami, A., 2015. Herpes simplex virus enhances chemokine function through modulation of receptor trafficking and oligomerization. Nat Commun 6, 6163.

Ostrove, J.M., Leonard, J., Weck, K.E., Rabson, A.B., Gendelman, H.E., 1987. Activation of the human immunodeficiency virus by herpes simplex virus type 1. J Virol 61, 3726-3732.

Polpitiya Arachchige, S., Henke, W., Pramanik, A., Kalamvoki, M., Stephens, E.B., 2018. Analysis of Select Herpes Simplex Virus 1 (HSV-1) Proteins for Restriction of Human Immunodeficiency Virus Type 1 (HIV-1): HSV-1 gM Protein Potently Restricts HIV-1 by Preventing Intracellular Transport and Processing of Env gp160. J Virol 92.

RC., W., 2001. Herpes Simplex Viruses, in: Knipe DM, H.P., Griffin DE, Lamb RA, Martin MA, Roizman B, Straus SE (Ed.), Fields Virology. Lippincott Williams&Wilkins, Philadelphia, New York, pp. 2461–2509.

Viejo-Borbolla, A., Martinez-Martin, N., Nel, H.J., Rueda, P., Martin, R., Blanco, S., Arenzana-Seisdedos, F., Thelen, M., Fallon, P.G., Alcami, A., 2012. Enhancement of chemokine function as an immunomodulatory strategy employed by human herpesviruses. PLoS Pathog 8, e1002497.

Xiang, Z., He, Y., 2013. Genome-wide prediction of vaccine targets for human herpes simplex viruses using Vaxign reverse vaccinology. BMC Bioinformatics 14 Suppl 4, S2.

Zhang, M., Liu, Y., Wang, P., Guan, X., He, S., Luo, S., Li, C., Hu, K., Jin, W., Du, T., Yan, Y., Zhang, Z., Zheng, Z., Wang, H., Hu, Q., 2015. HSV-2 immediate-early protein US1 inhibits IFN-beta production by suppressing association of IRF-3 with IFN-beta promoter. J Immunol 194, 3102-3115.

Figure legends

Fig. 1. Knockout of gJ results in impaired HSV-2 production in different cell types. The BAC DNA was transfected into Vero cells to produce gJ-null HSV-2 (named DelgJ HSV-2-GFP) and wild-type HSV-2 (WT HSV-2-GFP). (A) The adsorption of DelgJ HSV-2-GFP and WT HSV-2-GFP were compared using relative quantitative PCR. HeLa cells were infected with DelgJ HSV-2-GFP or WT HSV-2-GFP for 1h at 4°C. (B) The entry of DelgJ HSV-2-GFP and WT HSV-2-GFP were compared on cell monolayers for 2h at 37°C. The viral genomic DNA in (A) and (B) were extracted and analyzed by monitoring HSV-2 IE protein ICP0 using relative quantitative PCR. The difference in ICP0 gene was calculated on the basis of $2^{-\Delta\Delta CT}$ values. (C) The viral yields of DelgJ HSV-2-GFP and WT HSV-2-GFP in different cell lines. Vero, ARPE-19, HeLa or SH-SY5Y cells were infected with DelgJ HSV-2-GFP or WT HSV-2-GFP at an MOI of 5 PFU/cell. The supernatants and cells were collected at 24 hours post infection (hpi) and the virus yields were measured by plaque assay. (D) The viral genomic DNA in the parallel samples of (C) were extracted and analyzed by monitoring HSV-2 IE protein ICP0 using relative quantitative PCR. The difference in ICP0 gene was calculated on the basis of $2^{-\Delta\Delta CT}$ values. (E) The expression level of gD in the parallel samples of (C) was determined by western blot where actin was used as a loading control. Molecular weight standards in kilodaltons are shown on the left. (F) The virus production of DelgJ HSV-2-GFP and WT HSV-2-GFP in human primary epithelial cells. Human primary epithelial cells isolated from human foreskin tissues were infected with DelgJ

HSV-2-GFP or WT HSV-2-GFP at an MOI of 5 PFU/cell. The supernatants and cells were collected at 24 hpi and the virus yields were measured by plaque assay. Data shown are mean ± SD of three independent experiments with each condition performed in triplicate (A, B, C, D and F). One representative experiment out of three is shown (E). “ns” represents not significant, * represents $P<0.05$ and ** represents $P<0.01$, *** represents $P<0.001$.

Fig. 2. One-step growth curves of DelgJ HSV-2-GFP and WT HSV-2-GFP. Vero (A), HeLa (B) and ARPE-19 (C) cells were infected with DelgJ-HSV-2GFP or WT-HSV-2GFP at an MOI of 5 PFU/cell. At 0, 6, 12, 18, 24, 30 and 36 hpi, cells and supernatants were harvested and the viral yields were tittered on Vero cells. Data shown are mean ± SD of three independent experiments with each condition performed in triplicate.

Fig. 3. shRNA knockdown of gJ results in decreased HSV-2 production. (A) The knockdown efficiency of gJ shRNA. Serial concentration gradients of retroviral vectors expressing gJ shRNA (1-4#) or control shRNA were used to treat HeLa cells transfected with pgJ-flag or pcDNA3.1. At 48 hours post transfection, the expression of gJ-flag was measured by western blot where actin was used as a loading control. GFP signal represents the transfection efficiency. Molecular weight standards in kilodaltons are shown on the left. One representative experiment out of three is shown. (B) HSV-2 production in the gJ shRNA or control shRNA treated cells. HeLa or

ARPE-19 cells transfected with retroviral vectors expressing #1 gJ shRNA or control shRNA followed by infection with HSV-2 strain G at an MOI of 5 PFU/cell. Supernatants and cells were collected at 24 hpi, and thereafter, the viral yield of samples was analyzed using plaque assays. Data shown are mean ± SD of three independent experiments with each condition performed in triplicate. ** represents $P<0.01$.

Fig. 4. Ectopic expression of gJ enhances the replication of both WT and gJ-null HSV-2. HeLa or ARPE-19 cells were transfected with pgJ-flag or pcDNA3.1 followed by infection with WT HSV-2-GFP or DelgJ HSV-2-GFP at an MOI of 5 PFU/cell. Supernatants and cells were collected at 24 hpi, and thereafter, the viral yield of samples was analyzed using plaque assays. (A) The viral yields produced by HeLa cells infected with WT HSV-2-GFP or DelgJ HSV-2-GFP. (B) The expression level of gD in the parallel samples of (A) was determined by western blot where actin was used as a loading control. Molecular weight standards in kilodaltons are shown on the left. (C) The viral yields produced by ARPE-19 cells infected with WT HSV-2-GFP or DelgJ HSV-2-GFP. (D) The expression level of gD in the parallel samples of (C) was determined by western blot where actin was used as a loading control. Molecular weight standards in kilodaltons are shown on the left. Data shown are mean ± SD of three independent experiments with each condition performed in triplicate (A and C). One representative experiment out of three is shown (B and D). ** represents $P<0.01$.

Fig. 5. HSV-2 gJ is important for plaque and syncytia formation. Vero and HeLa cells were infected with DelgJ HSV-2-GFP or WT HSV-2-GFP at an extremely low MOI (~80 PFU/1×10^6 cells). In parallel, VgJ2 or HgJ2 cells were infected with RgJ HSV-2-GFP at a low MOI (~80 PFU/1×10^6 cells). After removal of the inoculum, cells were maintained in growth medium with anti-HSV-2 antibody (Abnova) at a dilution of 1:1000 to neutralize extracellular HSV-2. Plaques and syncytia formation were photographed and the plaque areas were compared after 48 h incubation at 37°C. (A) The morphology of plaques on Vero and VgJ2 monolayers infected with WT HSV-2-GFP, DelgJ HSV-2-GFP or RgJ HSV-2-GFP. (B) The statistics of relative plaque area on Vero and VgJ2 monolayers infected with WT HSV-2-GFP, DelgJ HSV-2-GFP or RgJ HSV-2-GFP. Data shown are mean ± SD of three independent experiments. “ ns” represents not significant, *** represents $P<0.001$. (C) Representative fields of plaque and syncytia formation acquired by fluorescence microscopy on Vero or HeLa monolayers infected with WT HSV-2-GFP or DelgJ HSV-2-GFP, and VgJ2 or HgJ2 monolayers infected with RgJ HSV-2-GFP. The green fluorescence represents HSV-2-infected cells. Nuclei were stained with Hoechst 33342 (blue). Representative confocal images from three independent experiments are shown. Scale bars in all panels represent 50 μm.

Fig. 6. HSV-2 gJ-mediated cell-to-cell spread leads to increased virus production. HeLa, ARPE-19 or SH-SY5Y cells were infected with DelgJ HSV-2-GFP or WT

HSV-2-GFP at very low MOI (~80 PFU/1×10^6 cells). In parallel, HgJ2, AgJ2 or SHgJ2 cells were infected with RgJ HSV-2-GFP at a low MOI (~80 PFU/1×10^6 cells). The ratio of GFP^+ cells, viral genomic DNA and virus production were compared after 48 h incubation at 37°C. (A) The ratio of GFP^+ cells in the HeLa, ARPE-19, SH-SY5Y, HgJ2, AgJ2 or SHgJ2 cells infected with DelgJ HSV-2-GFP, WT HSV-2-GFP or RgJ HSV-2-GFP was analyzed by flow cytometry. (B) The viral genomic DNA of the parallel samples of (A) was detected by relative quantitative PCR. (C) The virus production of the parallel samples of (A) was detected by plaque assay. Data shown are mean ± SD of three independent experiments with each condition performed in triplicate. "ns" represents not significant, ** represents P<0.01, and *** represents P<0.001.

Fig. 7. HSV-2 gJ promotes cell-to-cell spread among epithelial cells or from epithelial to neuronal cells. HeLa or ARPE-19 cells were infected with the same amount of DelgJ HSV-2-GFP or WT HSV-2-GFP at an MOI of 10 for 2h. In parallel, HgJ2 and AgJ2 cells were infected with RgJ HSV-2-GFP at an MOI of 10 for 2h. After digestion by trypsin, 100 cells per samples were taken out followed by co-cultivation with HeLa, ARPE-19, HgJ2, AgJ2, SH-SY5Y or SHgJ2 cells which were labeled with CellTracker Blue fluorescence dye for 2 days. HSV-2 transmission from infected to uninfected cells was subsequently quantified by flow cytometry. The CellTracker $Blue^+$ GFP^+ populations represent the newly infected cells. (A) HSV-2 transmission from infected HeLa to uninfected HeLa cells or from infected HgJ2 to

uninfected HgJ2 cells was quantified by flow cytometry. (B) The ratio of the CellTracker Blue^{+} GFP^{+} populations from three independent experiments. (C) The virus production in the parallel samples of (B) was determined by plaque assay. (D) HSV-2 transmission from infected ARPE-19 to uninfected ARPE-19 cells or from infected AgJ2 to uninfected AgJ2 cells was quantified by flow cytometry. (E) The ratio of the CellTracker Blue^{+} GFP^{+} populations from three independent experiments. (F) The virus production in the parallel samples of (E) was determined by plaque assay. (G) HSV-2 transmission from infected ARPE-19 to uninfected SH-SY5Y cells or from infected AgJ2 to uninfected SHgJ2 cells was quantified by flow cytometry. (H) The ratio of the CellTracker Blue^{+} GFP^{+} populations from three independent experiments. (I) The virus production in the parallel samples of (H) was determined by plaque assay. Data shown are mean ± SD of three independent experiments with each condition performed in triplicate (B, C, E, F, H and I). One representative experiment out of three is shown (A, D and G). "ns" represents not significant, * represents P<0.05, ** represents P<0.01, and *** represents P<0.001.

Fig. 8. HSV-2 gJ likely functions as a regulator to increase viral protein expression and virus production. (A) HSV-2 gJ enhances the expression of HSV-2 immediate early proteins ICP0, ICP22, ICP27 and late protein gB. 293T cells were cotransfected with pcDNA3.1, pgL-flag or pgJ-flag together with plasmid expressing immediate early proteins ICP0, ICP22, ICP27 or late protein gB. The expression level of ICP0-flag, ICP22-flag, ICP27-flag and gB in gJ-flag, gL-flag or control pcDNA3.1

transfected cells was measured by western blot where actin was used as a loading control. Molecular weight standards in kilodaltons are shown on the left. (B) The correlation between the dose of gJ and the expression level of ICP27 was analyzed by western blot where actin was used as a loading control. Molecular weight standards in kilodaltons are shown on the left. (C) The expression level of p24 in supernatants and cell lysates was detected by ELISA. 293T cells were cotransfected with pcDNA3.1, pgL-flag or pgJ-flag together with plasmid containing HIV-1 genome (pNL4-3). At 48h post transfection, supernatants and cells were harvested separately. The expression level of p24 in supernatants and cell lysates was detected by ELISA. (D) HIV-1 production in supernatants was analyzed in an infection assay using supernatants containing HIV-1 to infect TZM-bl cells. (E) The expression level of NS3 in gJ-expressing cells, gL-expressing cells or control cells. 293T cells were cotransfected with plasmid expressing JEV NS3 and pcDNA3.1, pgL-flag or pgJ-flag. At 24h post transfection, the expression level of NS3 in cell lysates was detected by western blot where actin was used as a loading control. Molecular weight standards in kilodaltons are shown on the left. (F) The virus production of JEV in gJ-expressing cells, gL-expressing cells or control cells. HeLa cells transfected with control pcDNA3.1, pgL-flag or pgJ-flag were infected with JEV at an MOI of 10 PFU/cell. At 24hpi, the viral yield was measured by plaque assay. One representative experiment out of three is shown (A, B and E). Data shown are mean ± SD of three independent experiments with each condition performed in triplicate (C, D and F). “ns” represents not significant, ** represents $P<0.01$ and *** represents $P<0.001$.

Figure 1

Click here to download high resolution image

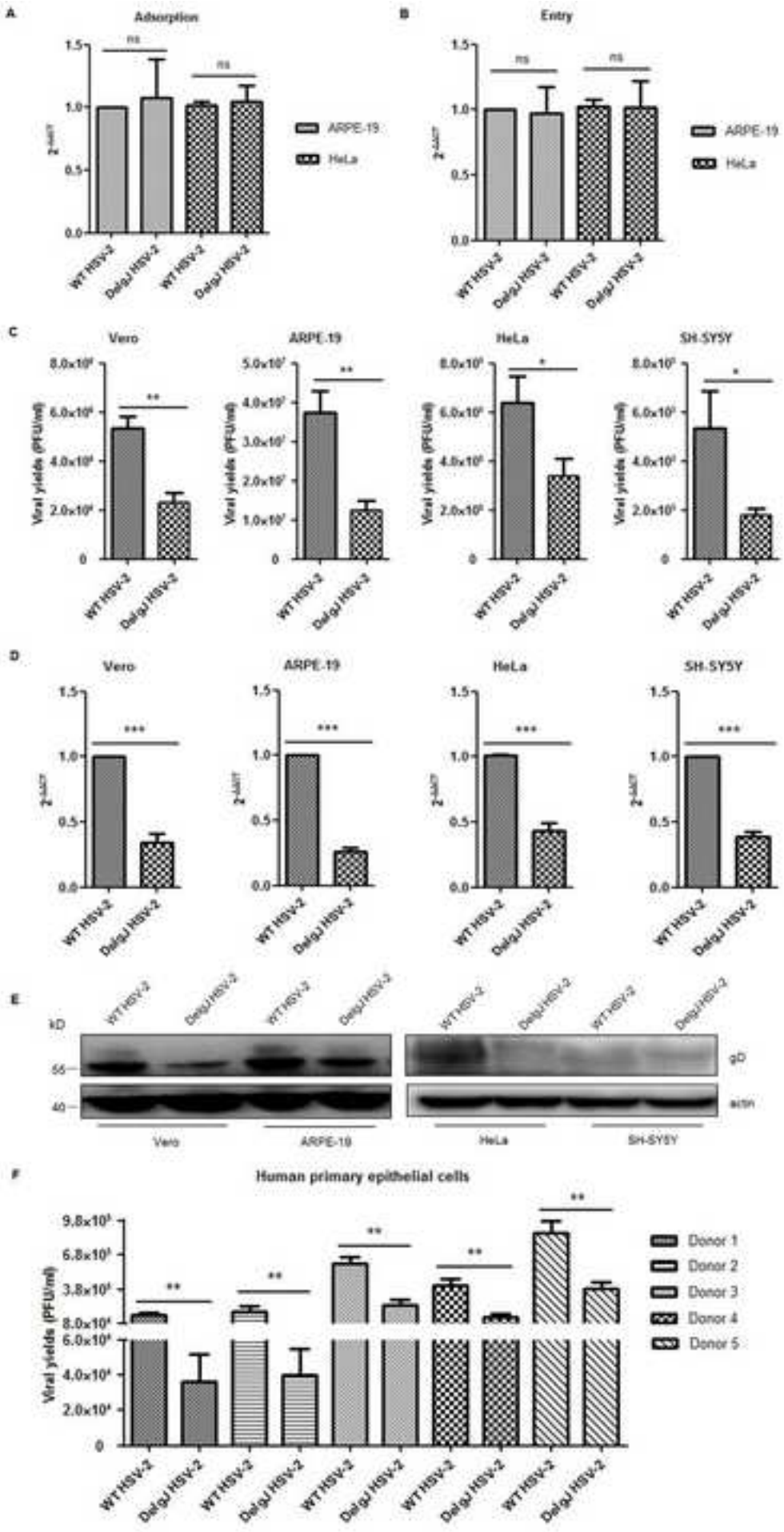

Figure 2

Click here to download high resolution image

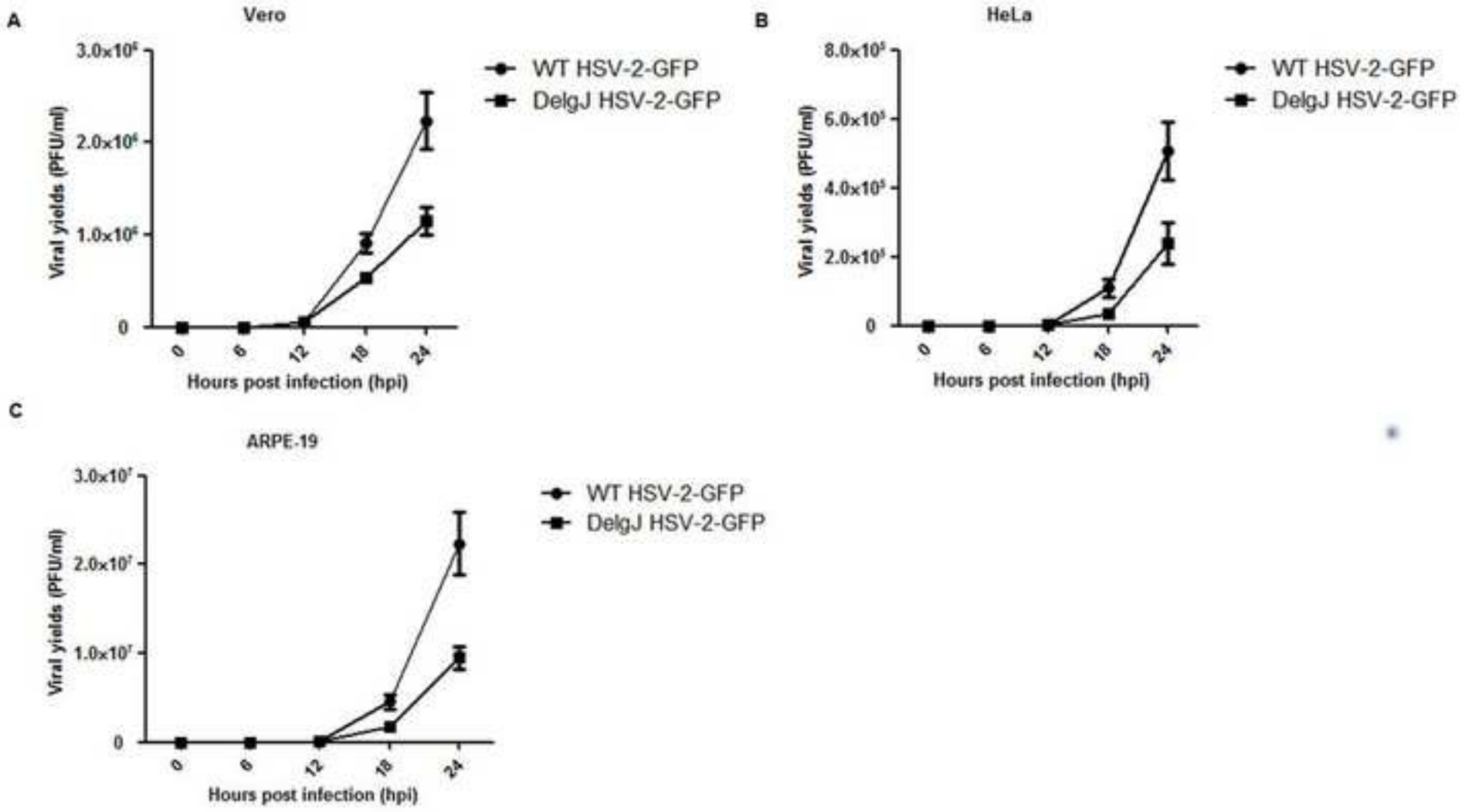

Figure 3

Click here to download high resolution image

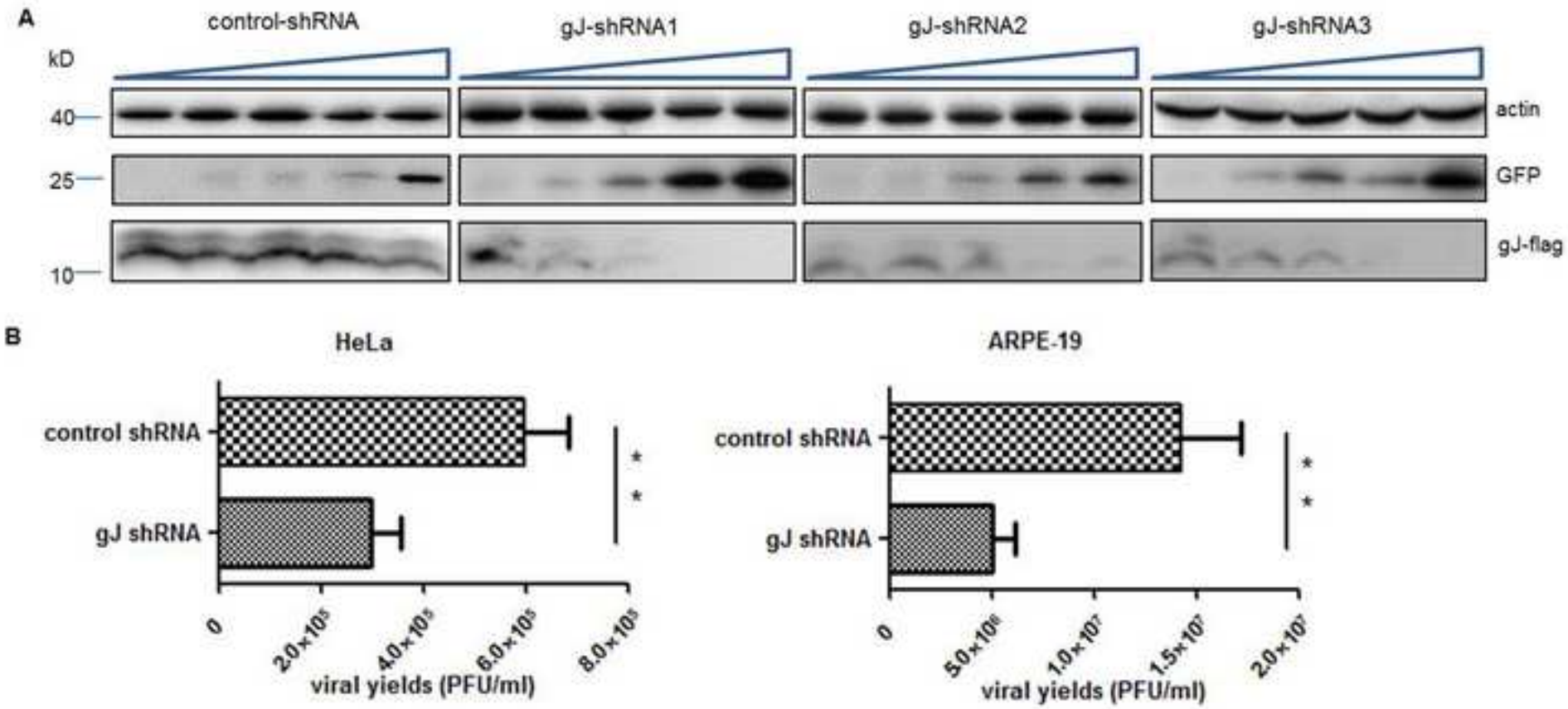

Figure 4

Click here to download high resolution image

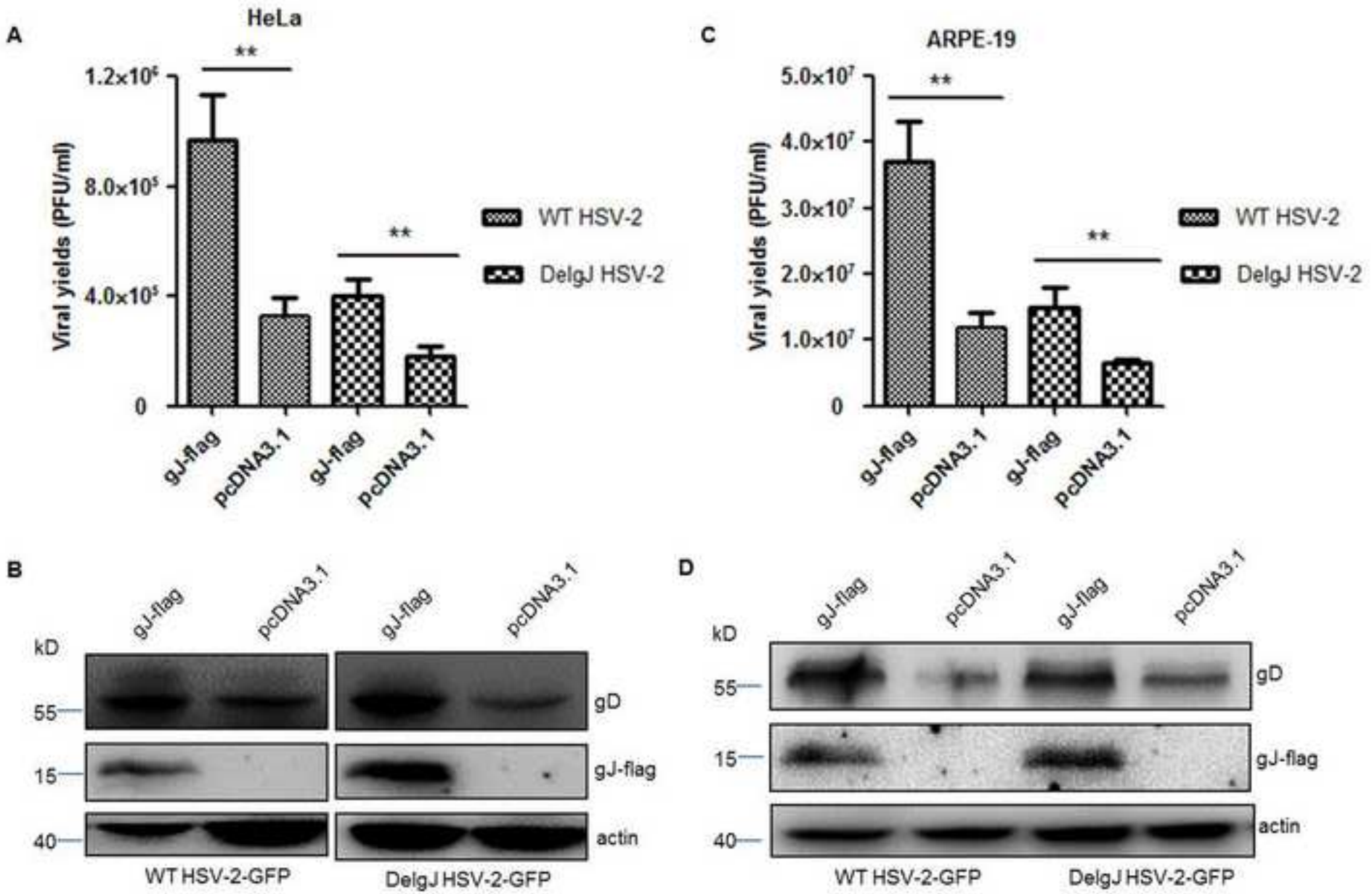

Figure 5

Click here to download high resolution image

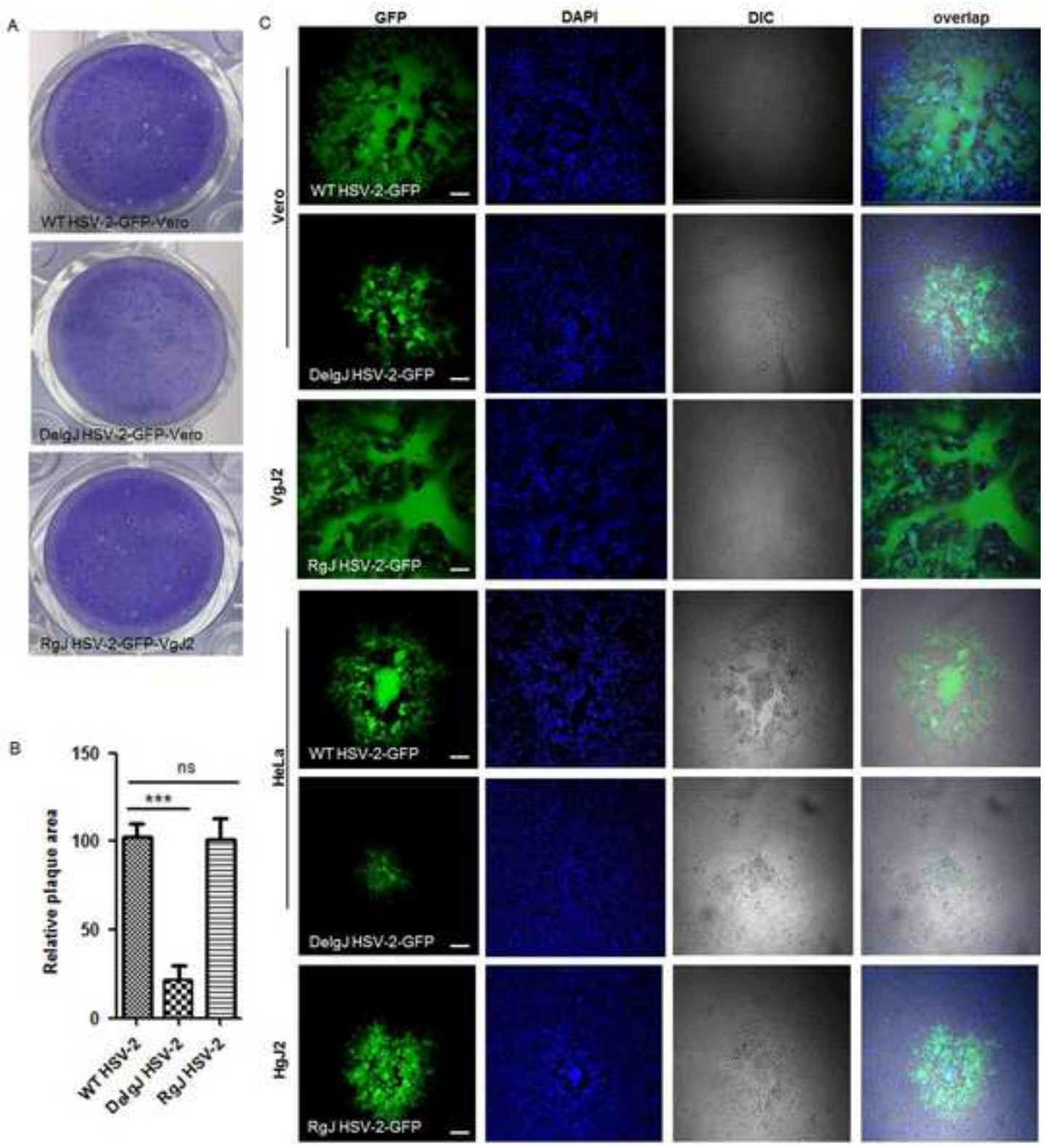

Figure 6

Click here to download high resolution image

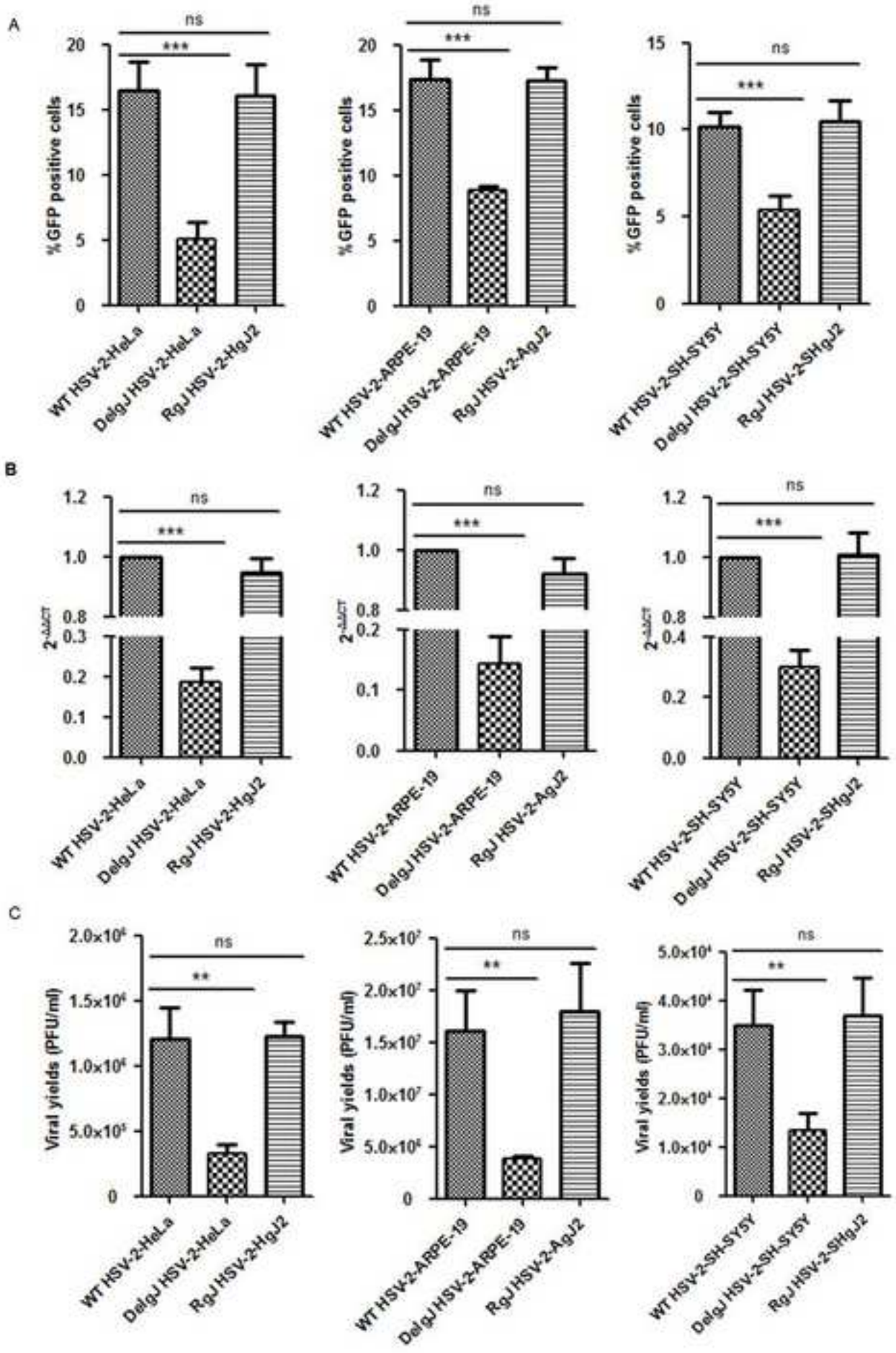

Figure 7

Click here to download high resolution image

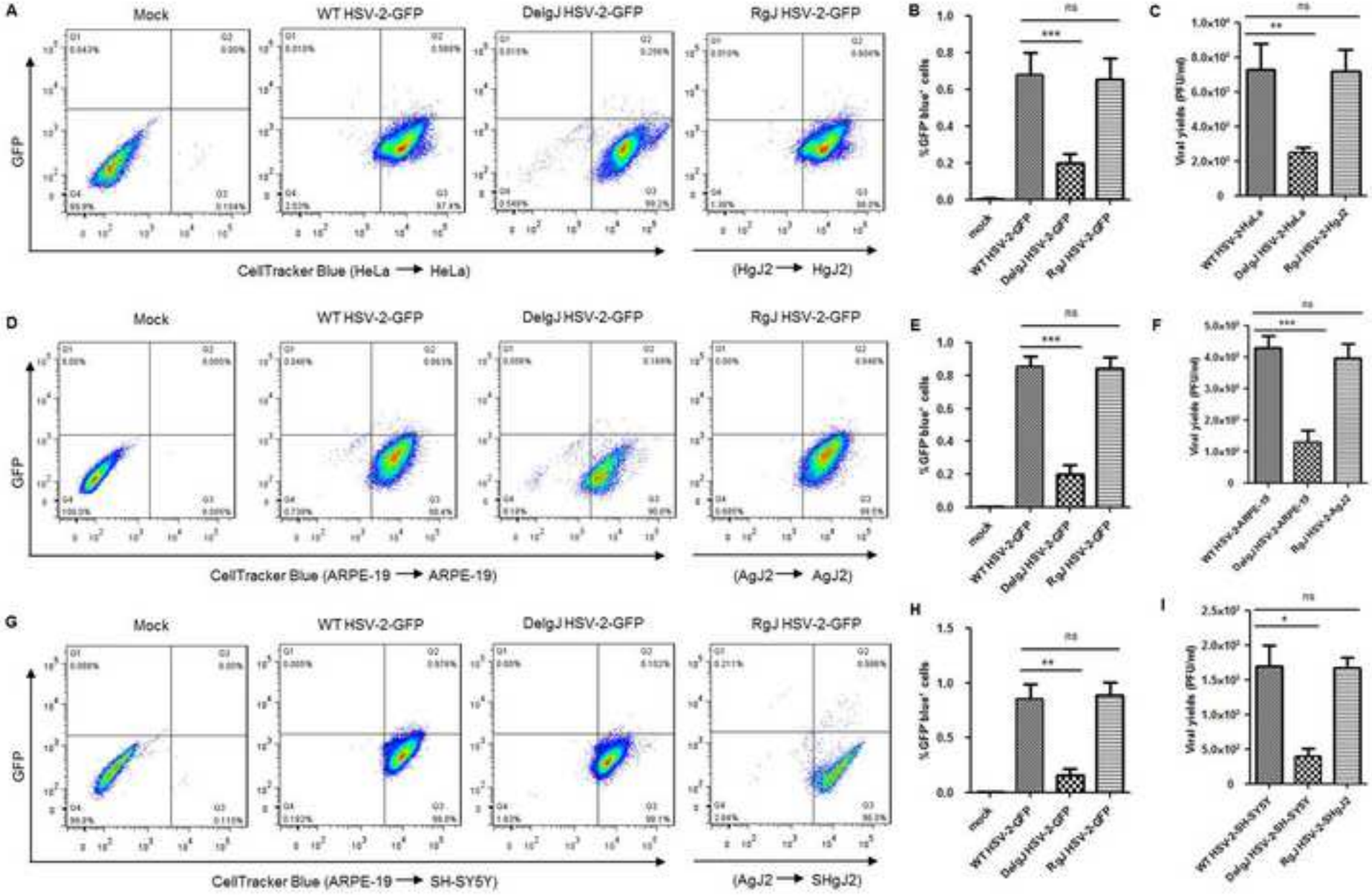

Figure 8

Click here to download high resolution image

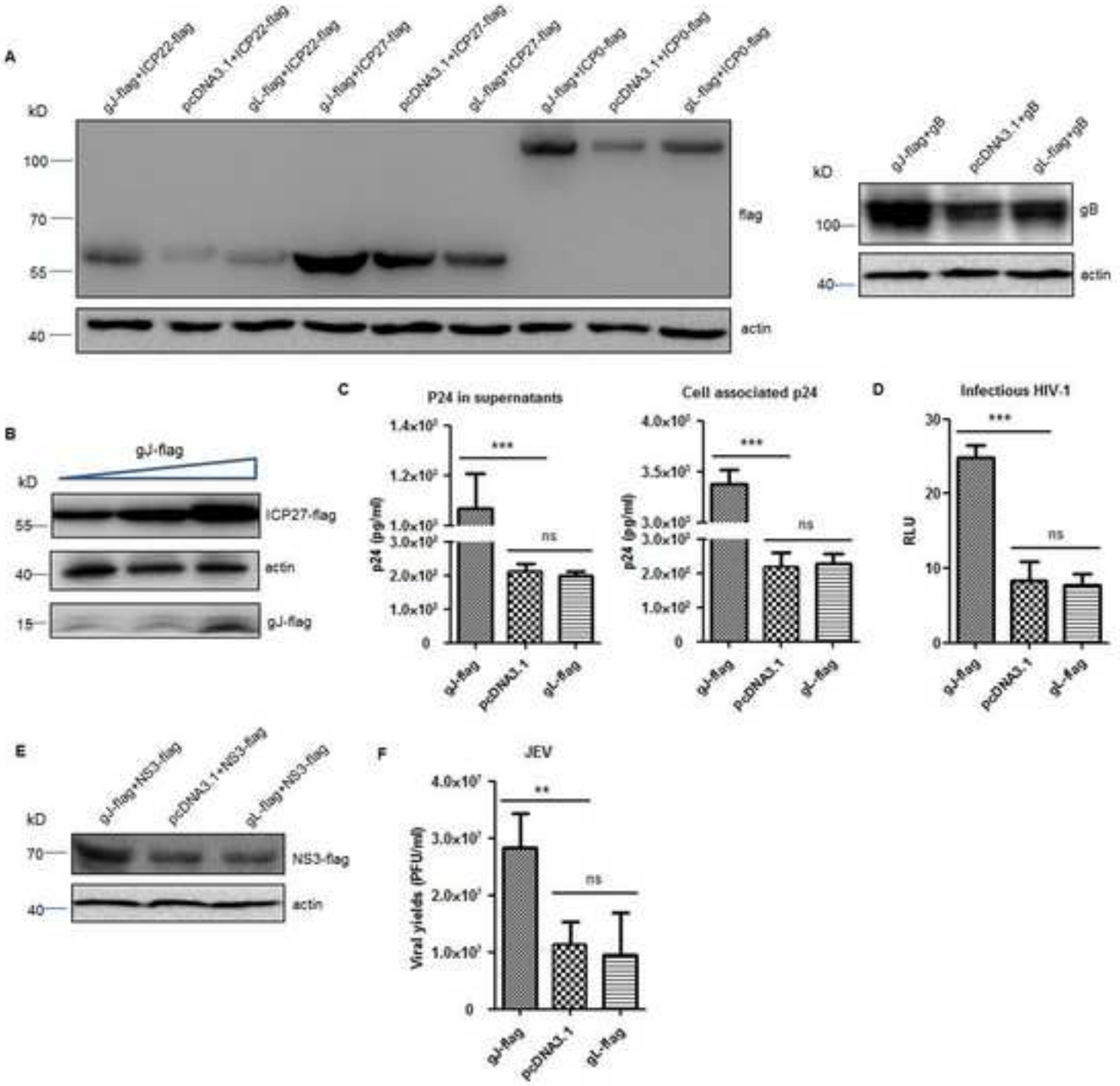

Supplementary Material (To be Published)

Click here to download Supplementary Material (To be Published): Supplementary materials.docx